THE ASTROPHYSICAL JOURNAL, 514:637–647, 1999 April 1

THE STARBURST-AGN CONNECTION IN ACTIVE GALAXIES: THE MASSIVE NUCLEAR STAR-FORMING DISK IN NGC 4303

L. COLINA[1,2]
Space Telescope Science Institute, Baltimore, MD 21218
AND
S. ARRIBAS
Instituto de Astrofísica de Canarias
Received 1998 August 19; accepted 1998 November 11

ABSTRACT

Two-dimensional spectroscopy of the low-redshift active galaxy NGC 4303 obtained with the Two-Dimensional Fiber ISIS System is presented. The ionization structure and velocity field of the nuclear region of this galaxy, where a compact UV-bright spiral structure connected with the UV-bright core has been detected with the *Hubble Space Telescope* (*HST*; Colina et al. 1997a), are investigated in detail. The ionized gas shows a structure similar to that observed in the high spatial resolution *HST* UV-continuum image. The Hβ and Hα emission is dominated by the nuclear star-forming regions, while the core of the galaxy is the brightest region in the [O III] λ5007 and [N II] λ6584 emission lines. The optical emission line ratios of the nuclear star-forming regions are characteristic of young (ages 2–3 Myr) star-forming regions, while the core of the galaxy shows the emission-line ratios of a low-luminosity AGN in between an [O I]–weak LINER and a low-excitation Seyfert 2. The nature of the ionizing source located at the core of the galaxy is still unsolved. Its luminosity and optical emission line ratios are compatible with the presence of a young ($\sim$3.5 Myr) massive ($\sim 8 \times 10^4\ M_\odot$) cluster of stars, but are also consistent with the existence of a power-law nonthermal ionizing source. Whatever the nature of this ionizing source, the nuclear star-forming spiral dominates the ionizing radiation, contributing about 90% of the total ionizing flux. The velocity field of the ionized gas, as measured by the Hβ emission line, is consistent with that of a massive rotating disk characterized by a radius of 300 pc, a rotation velocity of 85 km s^{-1}, an inclination of 45° with respect to the line of sight, and a kinematic major axis oriented along P.A. 130°. The inferred dynamical mass inside a radius of 300 pc is $5.0 \times 10^8\ M_\odot$. The mass and size of this nuclear rotating disk is similar to those recently detected in ultraluminous infrared galaxies like Mrk 231 and Arp 220. The observed line profiles of the high-excitation [O III]–emitting gas show the presence of two kinematically distinct gaseous components. The main component follows the velocity pattern of the massive rotating disk. The secondary component has an amplitude of $\pm$350 km s^{-1}, and a minor axis oriented, in projection, almost perpendicular to the minor axis of the low-ionization gas. This second [O III] velocity component could represent gas located in a nuclear ionizing cone, i.e., gas flowing outward outside the plane of the low-excitation gas disk, and being ionized by the UV-bright source located at the core of the galaxy. The proximity of NGC 4303 together with the detection of (1) an AGN-like nucleus, (2) a compact nuclear star-forming spiral structure connected to the nucleus, (3) a massive rotating nuclear disk, and (4) radially flowing high-excitation gas makes this galaxy an ideal candidate for the study of the fueling of active galaxies and the starburst-AGN connection.

Subject headings: galaxies: active — galaxies: individual (NGC 4303) — galaxies: kinematics and dynamics — galaxies: spiral — galaxies: starburst

1. INTRODUCTION

Three major questions have been the subject of intense investigations in the area of active galaxies over the past several years and are still largely unsolved: (1) what mechanisms trigger nuclear starbursts in galaxies? (2) How are active galactic nuclei (AGNs) nourished? And (3) is there any connection between nuclear starbursts and AGNs?

The first two questions have been addressed by numerical simulations of the effects of bars in spiral galaxies (Shlosman, Frank, & Begelman 1989, hereafter SFB89; Shlosman, Begelman, & Frank 1990, hereafter SBF90). According to these models, bars are an efficient mechanism for channeling gas from the outer to the nuclear regions in spirals. Gas is piled up at the distances of the inner Linblad resonances (ILRs), and star-forming rings are created (NGC 4321, Knapen et al. 1995; NGC 4314, Benedict, Smith, & Kenney 1996; NGC 3351, Colina et al. 1997a). If gas still flows inward, it would create a disk of gas that, if massive enough, would become unstable. Under this scenario, the nucleus could be fed and eventually turn into an AGN (SFB89; Fukuda, Wada, & Habe 1999). The existence of such massive nuclear disks of gas has recently been inferred from interferometric CO maps in the ultraluminous infrared galaxies Arp 220 (Scoville, Yun, & Bryant 1997) and Mrk 231 (Bryant & Scoville 1996).

The question of whether or not nuclear starbursts and AGNs are connected has been tackled by several authors suggesting that AGNs could be the final stage in the evolution of a nuclear starburst (Weedman 1983; Shapiro & Teu-

[1] Affiliated with the Astrophysics Division, Space Science Department, ESA.

[2] Current address: Instituto de Fisica de Cantabria, Facultad de Ciencias, Avda. de los Castros S/N, Santander, Spain. On leave from the Department of Astronomy and Astrophysics, University of Valencia, Spain.

kolsky 1985; Norman & Scoville 1988). These models predict that a central cluster of stars will evolve, collapse into a black hole, and ultimately generate an AGN. Other authors (Terlevich et al. 1994) suggest that different types of AGNs are, in fact, manifestations of different phases in the evolution of a star cluster located in the high-density, high-metallicity environment present in the core of early-type spiral galaxies. The direct evidence that nuclear or circumnuclear star-forming regions exist and dominate the observed UV emission in several Seyfert 2 galaxies has recently been provided by several authors using the *Hubble Space Telescope* (*HST*) and/or ground-based observations (Colina et al. 1997b; Heckman et al. 1997; Gonzalez-Delgado et al. 1998).

The structure of nuclear starbursts, their velocity fields, the existence of radial flows, the presence of a massive nuclear disk of gas, the role of the different sources of ionization, and, in general, the starburst-AGN connection in active galaxies, including luminous infrared galaxies, can be investigated in detail by means of two-dimensional field spectroscopy of a sample of nearby spirals with previously identified circumnuclear starbursts, some of them already known to have an AGN.

NGC 4303 is one such galaxy classified as a SAB(rs)bc spiral (de Vaucouleurs et al. 1991), located in the Virgo cluster and with a known compact starburst (Pogge 1989). Optical spectra of NGC 4303 through large apertures indicate that this galaxy harbors a nuclear starburst and a LINER or Seyfert 2 nucleus (Filippenko & Sargent 1986; Kennicutt, Keel, & Blaha 1989). Recent high–spatial resolution *HST* UV images of NGC 4303 (Colina et al. 1997a) show, for the first time in an active galaxy, the presence of a compact UV-bright spiral structure of about 240 pc in radius and connected with the unresolved AGN-like core.

In this paper we present the results of a two-dimensional fiber spectroscopy study of NGC 4303. This technique is specially suited for the study of the nuclear region of this complex and spectrally rich galaxy, since it *simultaneously* provides spatial and spectral coverage (see, e.g., Arribas et al. 1997, and references therein), and therefore allows a complete study of the kinematics and excitation conditions. Section 2 explains the observations and the specific reductions needed for this type of observation. Section 3 presents the results, including the continuum and emitting gas distributions (§ 3.1), the excitation conditions (§ 3.2), and the kinematics of the ionized gas (§ 3.3). Section 4 discusses the results and its implications, in particular the presence of different sources of ionization and their contribution to the total luminosity of the nuclear regions (§ 4.1), the detection of a massive nuclear rotating disk (§ 4.2), the implications for the fueling of active galaxies and the bar-starburst-AGN scenario (§ 4.3), the implications for the study of ultraluminous infrared galaxies (§ 4.4), and the detection of radial flows and, possibly, an ionizing cone (§ 4.5).

In this paper we define the core of the galaxy as the unresolved emitting region located at the center of the observed structure (with a size less than 8 pc, according to the *HST* UV image), and as nuclear regions any of the compact UV-continuum and/or emission-line emitting regions located outside the core but within a radius of 300 pc from it. For NGC 4303, we adopt the distance of M100, the brightest spiral in the Virgo cluster (16.1 Mpc; Ferrarese et al. 1996; $1'' = 78$ pc).

2. OBSERVATIONS AND DATA REDUCTION

The data analyzed in this paper were obtained on 1997 February 12 and 13 at the Observatorio del Roque de los Muchachos on the island of La Palma. We used the Two-Dimensional Fiber ISIS System (2D-FIS), which links the f/11 Cassegrain focus of the 4.2 m William Herschel Telescope (WHT) with the ISIS double spectrograph. A detailed technical description is provided by García et al. (1994); here we only recall its main characteristics. The core of the system consists of a 2.5 m long bundle formed by 125 optical fibers, each 200 μm in diameter (0.″9 on the sky), arranged in two groups at the focal plane. One has 95 fibers, forming an array 9.″4 × 12.″2 on the sky, and the other has 30 fibers forming a ring 38″ in radius and are intended for collecting the sky background light in the case of small-sized objects. The relative positions of the fibers at the telescope's focal plane are known very accurately, being the distance between two adjacent fibers, as about 1.″1. At the slit the fibers are arranged linearly (with a distance of 425 μm between adjacent fibers). With this type of arrangement, a set of spectra—corresponding to 125 zones in the circumnuclear region—is recorded in each exposure. The advantage of the system as opposed to, say, a Fabry-Pérot interferometer is that all of the spectral and spatial information is recorded simultaneously, and the limits on the spectral coverage are imposed by the spectrograph alone. Details on the technique itself may be found in Arribas, Mediavilla, & Rasilla (1991), and references therein.

The observations were made by simultaneously using the blue and red arms of the double spectrograph ISIS (Carter et al. 1993). In the blue arm, a 600 groove mm^{-1} grating allowed high-resolution spectroscopy ($\sim$1.5 Å) in the spectral range 4490–5300 Å. With a 158 groove mm^{-1} grating, a lower resolution ($\sim$5 Å), but a larger spectral range (5750–8960 Å), was obtained in the red arm. With the above configuration two consecutive exposures of 1800 and 900 s, respectively, were taken for the central region of NGC 4303. Clouds reduced the efficiency of the entire system during some periods of time. The autoguiding could be maintained, however, but the absolute flux calibration of the data cannot be achieved.

The reduction process consists of two main steps: (1) reduction of the spectra themselves, and (2) generation of continuum and emission-line images from the reduced spectra.

Since the spectra appear well-separated on the detector, step (1) is basically done in the same way as for long-slit spectroscopy, including the dark and flat-field corrections and the wavelength calibration. The rms of the polynomial fit to the arc line positions are 0.15 and 0.25 Å for the blue and red spectral range, respectively. These values are equivalent to about 9 km s^{-1} ([O III] λ5007) and 12 km s^{-1} (Hα). The sky background is obtained from the outer ring of fibers. However, the spectra of some of these fibers show emission lines from the galaxy (e.g., Hα), and these are excluded before the subtraction is performed. The final reduced spectra of the central 95 fibers centered on the Hβ, [O III] λ5007, Hα–[N II] $\lambda\lambda$6548, 6583, and [S II] $\lambda\lambda$6716, 6731 lines are presented in Figures 1*a*–1*d*.

To obtain two-dimensional maps of any feature (e.g., continuum, line intensity, velocity shifts, etc.) derived from the individual spectra (step [2]), a file with the x and y positions of the fibers at the telescope focal plane and the spectral

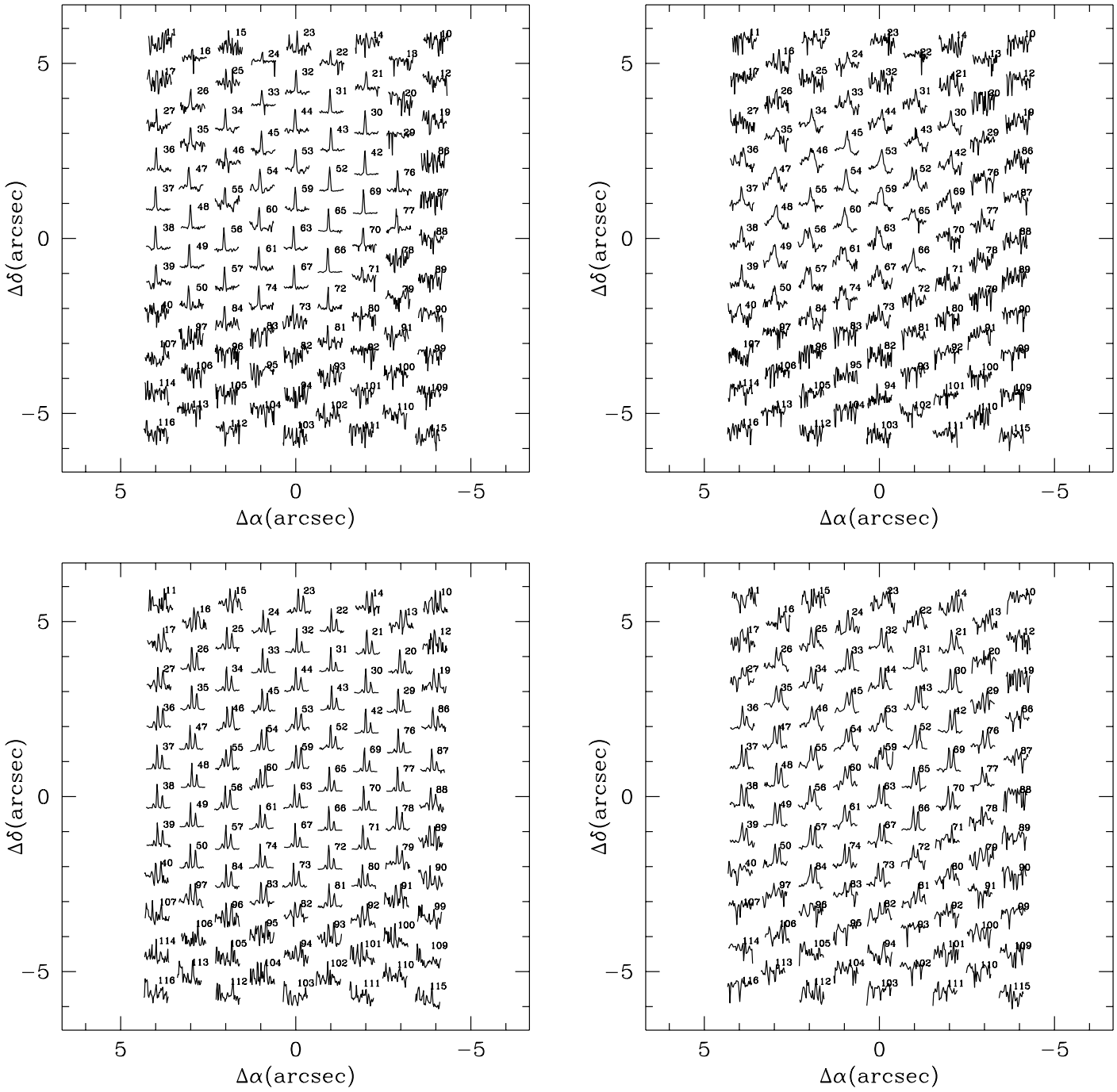

FIG. 1.—Plots presenting the final calibrated profiles of several emission lines including (*top left-hand panel*) Hβ, (*top right-hand panel*) [O III] λ5007, (*bottom left-hand panel*) Hα + [N II] $\lambda\lambda$6548, 6584, and (*bottom right-hand panel*) [S II] $\lambda\lambda$6717, 6731. The bundle of fibers covers a projected size of 9″ × 12″ on the sky, and the numbers in the plot indicate the number of the fiber in the bundle (position at the slit).

feature is generated. This file is then transformed into a regularly spaced rectangular grid, building up images of 51 × 51 pixels, with a scale ∼0.″3 pixel^{-1}. When creating a continuum map, an emission-line–free *filter* is defined to obtain the total emission on the selected wavelength range. The line intensity maps presented here are obtained in a similar manner after subtraction of the nearby continuum map. For this type of map, flat corrections (using flat exposures) are applied in order to homogenize the fiber sensitivity. Errors in this correction are small (∼5%) and are irrelevant for the study of the velocity fields.

By comparing red and blue continuum images of the standard stars, a relative offset between these images is found, which is mostly due to differential atmospheric refraction. After correcting by this effect (taken as reference Hα), some residual offset amounting to about 0.″2–0.″3 is obtained, which gives a good estimate of the uncertainty in the positioning.

To estimate the effective seeing during the observations, images of the star HD 132737 were obtained with the same detector configuration just before the observations of the galaxy were taken. The measured FWHM of these images is

1″.4, and although the exposure time for the images of the galaxy is longer, a significant degradation of the effective seeing is not expected, since the guiding system of the WHT is excellent.

3. RESULTS

3.1. *Stellar and Ionized Gas Distributions*

The stellar distribution in the nuclear region of NGC 4303 is traced by true continuum images generated selecting emission-free windows (centered at 4700, 6100, and 8225 Å, respectively) in the 2D-FIS spectra (see Fig. 2, where the *HST* UV image at 2200 Å is also shown for comparison).

The blue image (4700 Å) shows a centrally peaked stellar distribution and a faint trace of the UV-bright nuclear regions detected in the *HST* image. The optical (6100 Å) and red (8225 Å) images show a centrally peaked light distribution with an elongation toward the west. This asymmetry decreases with wavelength in agreement with recent ground-based *J*- and *K*-band images of NGC 4303 (Elmegreen et al. 1997).

The presence of very distinct and bright nuclear regions in the UV that almost vanish at red and near-infrared wavelengths is most likely an indication that these regions are young and active star-forming regions where massive stars have not even reached the red supergiant phase, i.e., ages are less than 5 Myr (see § 4.1 for a more detailed discussion).

The overall structure of the ionized gas is traced by the images of the low- and high-excitation line-emitting regions. These images are constructed from the 2D-FIS spectra selecting the appropriate wavelength windows centered on the emission lines and after subtraction of the corresponding nearby continuum (Fig. 3, where the *HST* UV image at 2200 Å is also shown for comparison).

The overall distribution of the ionized gas, best traced by the Hα emission line, clearly shows the existence of a faint Hα-emitting region in the core of the galaxy (i.e., central 1″ in size), and the presence of bright compact Hα-emitting regions distributed along the spiral-like structure previously observed in the UV (Colina et al. 1997a). In addition, the [S II] λλ6717, 6731 image shows the presence of a more diffuse ionized gas component covering the entire nuclear region (i.e., 2″–3″ in radius). If a circular geometry is assumed, the observed ionized gas structure corresponds to that of a disk inclined by 45° with respect to the line of sight and with a photometric major axis along P.A. 130°. The

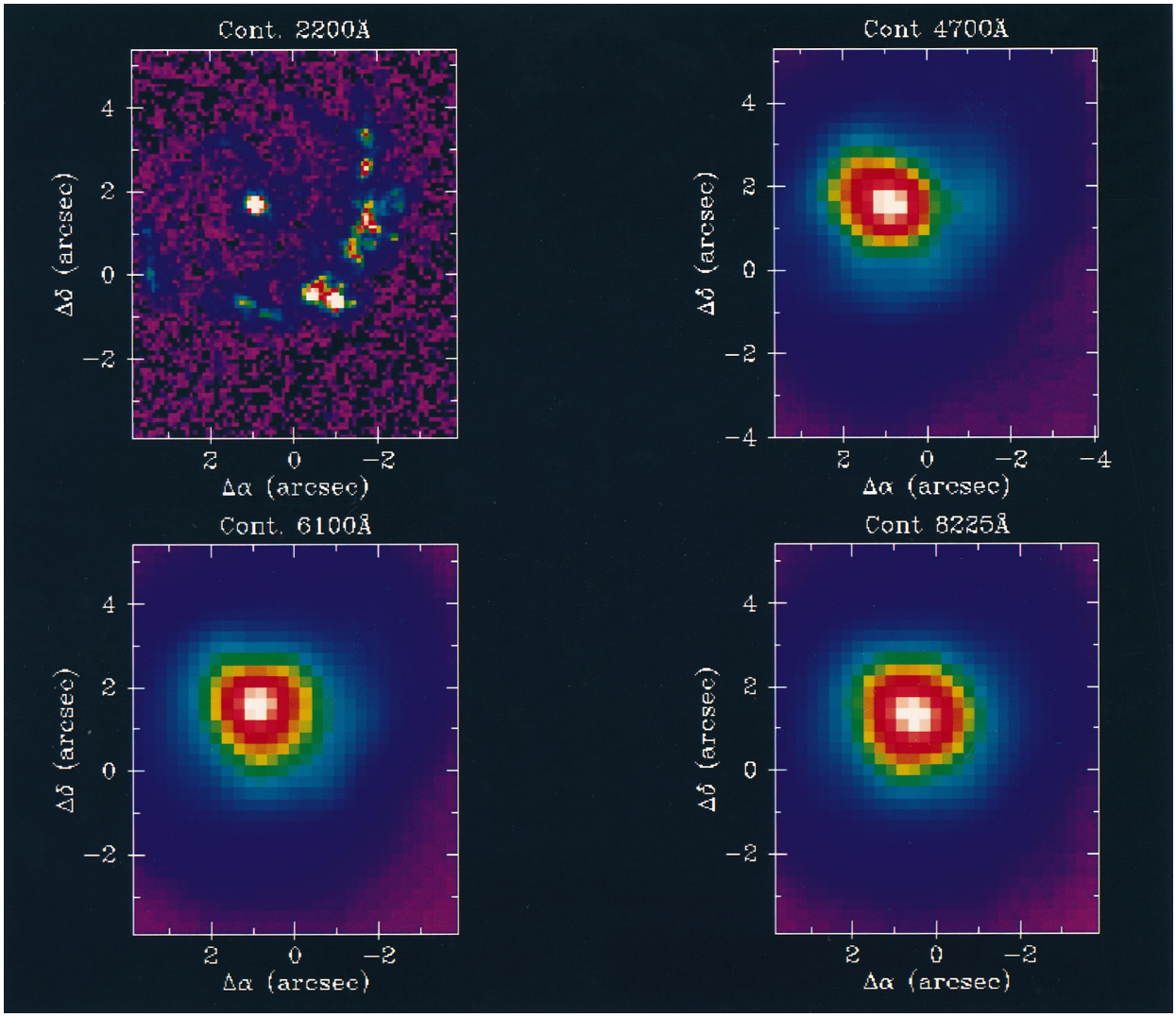

FIG. 2.—Images of the nuclear region of NGC 4303 in emission-line–free continuum light. The high-resolution *HST* UV image (Colina et al. 1997a) is also shown for comparison. The UV-bright star-forming spiral can also be traced in the blue light (4700 Å), but it shows up as a decreasing asymmetry in the light distribution at longer wavelengths.

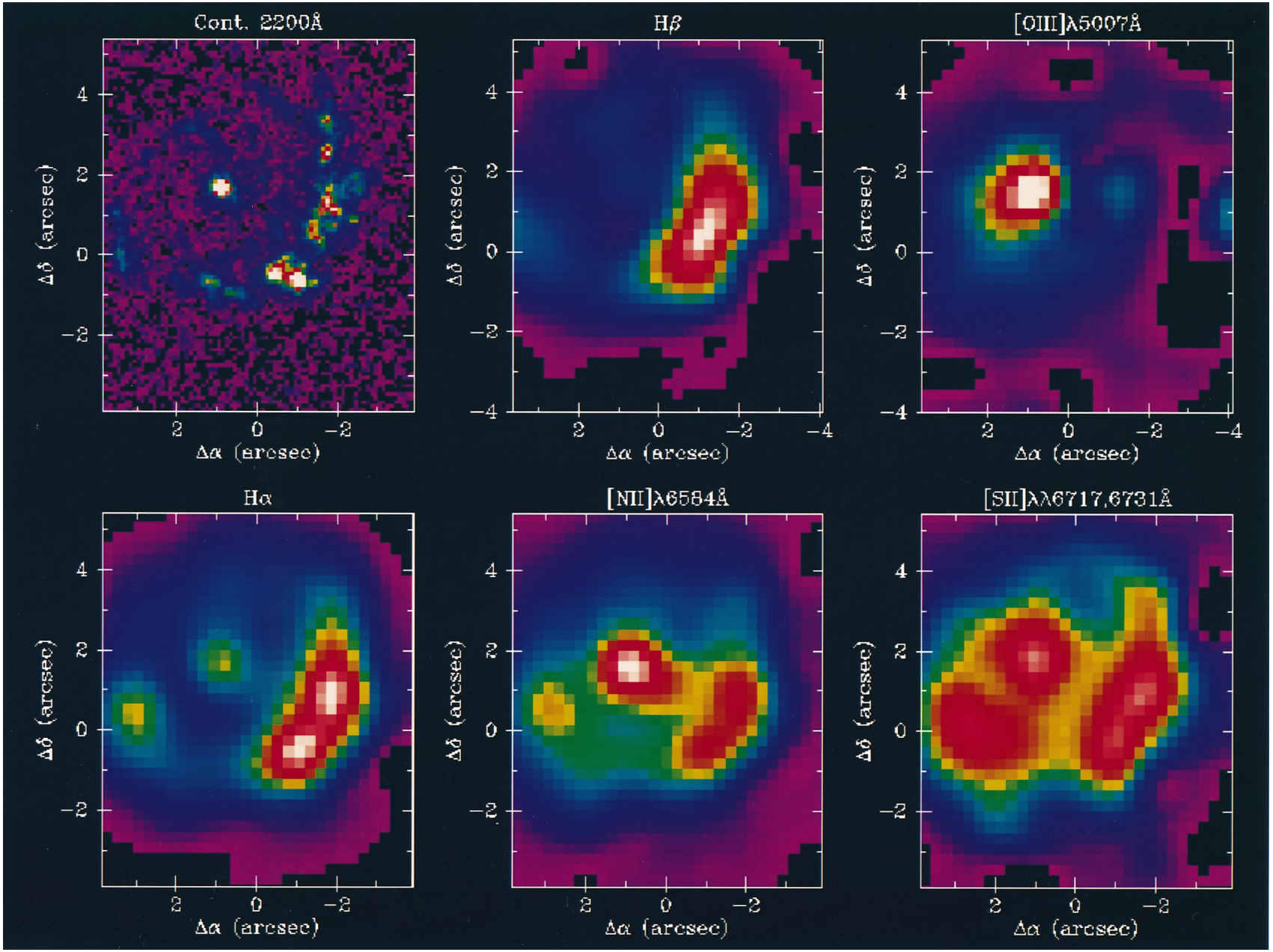

FIG. 3.—Images of the ionized gas in the nuclear region of NGC 4303 as traced by different emission lines. The high-resolution *HST* UV image (Colina et al. 1997a) is also shown for comparison. Differences in the excitation conditions are clear, with the core of the galaxy being the brightest [O III] λ5007 and [N II] λ6584 source. The Hα, and therefore the ionizing flux, is dominated by the nuclear star-forming regions, while the core dominates the [O III] emission.

image of the [O III] λ5007 emission line shows the presence of an additional faint [O III]–emitting region about 2″ west of the nucleus (Fig. 3), but with no clear correspondence with any of the bright Hα- or UV-emitting regions; i.e., no trace of a local ionization source. Thus this region could represent gas being directly ionized by the UV-bright ionizing source located at the core of the galaxy and related with a secondary [O III] kinematic component detected around the core (see § 3.3.2).

3.2. *Excitation of the Ionized Gas and Differential Extinction*

The bright compact Hα-emitting regions have a 1:1 correspondence with the UV-bright regions (see Fig. 3). However, there is a clear distinction between the UV- and Hα-emitting regions: the core of the galaxy, which in the UV is a factor 2–3 brighter than the brightest nuclear UV-bright regions (Colina et al. 1997a), appears as a relatively faint Hα source with a flux 2.5 times fainter than the brightest nuclear Hα regions (R1 and R2 in Table 1). An even more extreme case is the region 2″ east of the nucleus. This region (R3 in Table 1) is about 10 times fainter than the core in the UV but has a comparable Hα flux. In summary, while the core of the galaxy emits about 50% of the observed UV flux emitted by all of the bright regions, it only contributes to about 15% of the observed Hα flux.

The excitation conditions of the ionized gas have been measured at four different positions coincident with the core of the galaxy and the three bright and well-separated regions detected in the UV and Hα images. For each region, the flux of the emission lines is measured using an aperture of 0.″5 in radius centered at the position of the emission peak. No corrections for internal extinction and lines in absorption (hydrogen Balmer lines) have been applied (see Table 1 for specific ratios).

The emission-line ratios measured in the brightest nuclear Hα-emitting regions are typical of low-excitation H II regions. The core itself shows excitation conditions different from those observed in the nuclear star-forming regions. In particular, the core dominates the [O III] emission, and it is the brightest [N II] source.

The combination of internal differential extinction and different ionization mechanisms are the most likely explanation for the changes observed in the emission-line ratios and in the distribution of the Hα light (i.e., ionizing photons) relative to the UV (see § 4.1 for a more detailed discussion).

3.3. *Kinematics of the Ionized Gas*

3.3.1. *Low Ionization Gas*

The kinematics of the low-ionization–emitting gas is traced by the Hβ emission line velocity field (Fig. 4; upper left-hand panel). This emission line is selected instead of the more intense Hα because, contrary to Hα, Hβ appears isolated and was recorded at a higher spectral resolution (see § 2). In addition, Hβ does not show clear evidence of substructure because of the integration along the line of sight of several gaseous components, although in some spectra this possibility cannot be discarded. The individual velocities from which the Hβ velocity field is generated are obtained by adjusting a single Gaussian function to the observed profiles. This is accomplished with the help of the DIPSO package (Howarth & Murray 1988), and an average velocity uncertainty of 6 km s^{-1} is achieved in the determination of the centroid of the emission line.

The heliocentric radial velocity for the nucleus, defined as the peak in the Hβ emission line distribution, is 1545 ± 15 km s^{-1}. This value is slightly different from the heliocentric systemic velocity inferred from radio measurements (1569 ± 3 km s^{-1}; de Vaucouleurs et al. 1991).

The velocity field shows a regular pattern with the kinematic axes rather well-defined at 130° (major) and 40° (minor), with an estimated uncertainty of ±5°. Their good agreement with the photometric axes inferred from the UV and Hα images strongly suggests that the Hβ velocity field represents rotational motions in a disk. The peak-to-peak amplitude of the observed velocity field is ∼150 km s^{-1}. This could be even larger, since it is not completely clear that velocity maxima are observed, although this seems to be the case at least in the red part of the velocity field (Fig. 4; upper left-hand panel).

3.3.2. *High Ionization Gas*

The [O III] λ5007 profiles (Fig. 1*b*) show substructure likely due to the integration along the line of sight of the emission coming from several kinematically distinct gaseous components. The [O III] line profiles are broader than Hβ, and in a number of spectra a clear splitting is observed (see panels 52, 59, 63, and 65 in Fig. 1*b*). This suggests the presence of at least two distinct velocity components emitting in [O III]. In fact, by adjusting two Gaussians to the observed [O III] profiles, reasonable good fits are obtained in most cases.

The results from these fits reveal that the [O III] main component follows the kinematics of the Hβ-emitting gas. In particular, comparing the radial velocities of this component and those inferred for Hβ, a mean difference of 21 ± 30 km s^{-1} is obtained. The secondary [O III] component indicates the presence of large (about −350, +350 km s^{-1}) radial velocities. The individual radial velocities associated with this component are relatively uncertain, but its general velocity field is well defined (Fig. 4; upper right-hand panel). The blue/red symmetry of this map is remarkable with respect to the nucleus being the kinematic major

TABLE 1

EMISSION-LINE RATIOS IN NGC 4303

Region (1)	Δα (2)	Δδ (3)	F_{UV}/F_{UV}^{core} (4)	Hα/Hα^{core} (5)	[O III]/Hβ (6)	[O I]/Hα (7)	[N II]/Hα (8)	[S II]/Hα (9)
Core	0.0	0.0	1.0	1.0	0.50	−0.96	0.01	−0.31
R1.....	−2.7	−0.8	0.6	2.2	−0.78	...	−0.33	−0.63
R2.....	−1.9	−2.1	0.4	2.1	−0.72	...	−0.35	−0.64
R3.....	2.0	−1.3	0.1	1.2	...	...	−0.19	−0.42
Total.....	...	...	2.1	6.5	−0.27	...	−0.23	−0.51

NOTE.—Cols. (6)–(9) represent the logarithm of the different optical emission line ratios

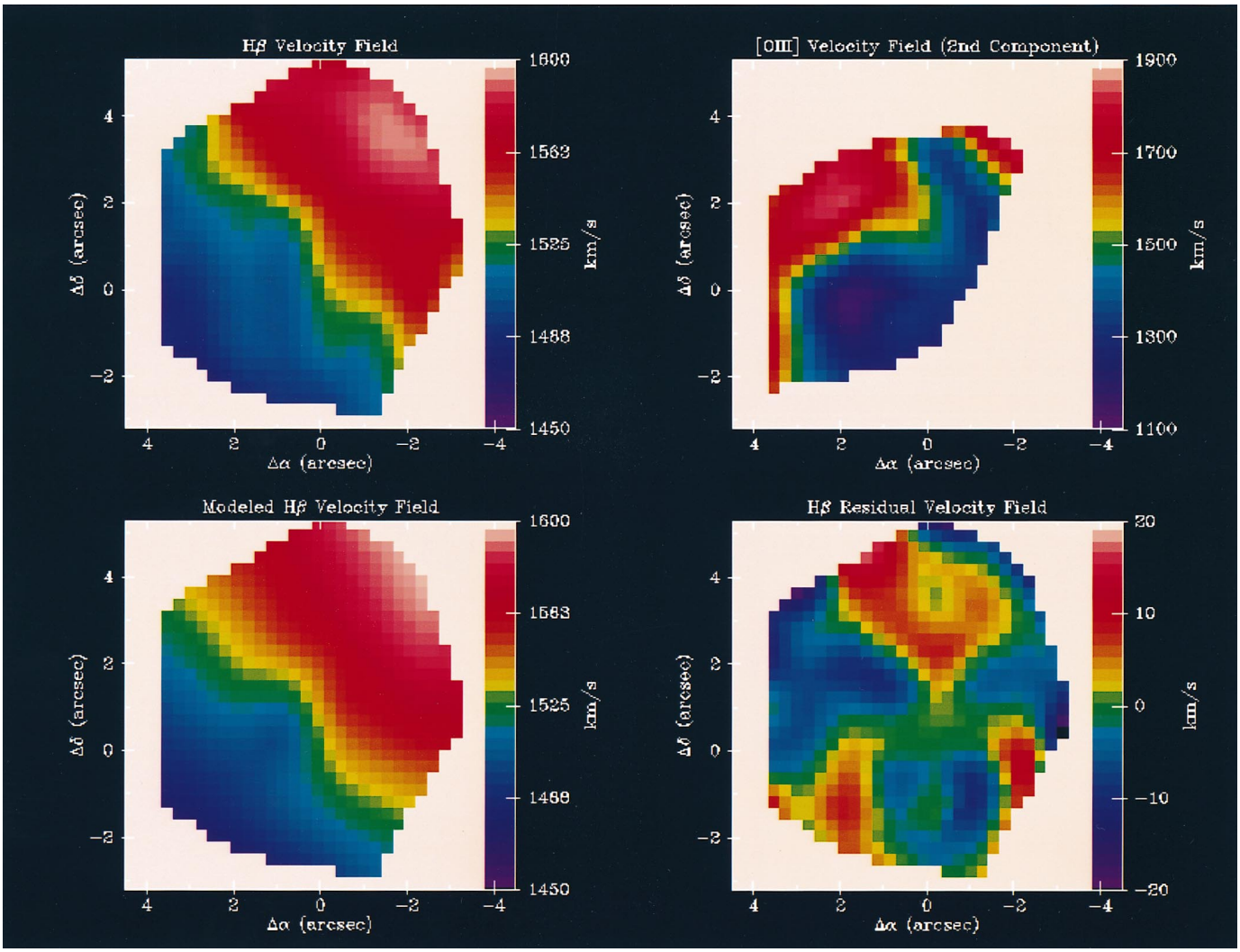

FIG. 4.—Images show the kinematic properties of the different components of the ionized gas in the nuclear region of NGC 4303. The overall velocity field of the ionized gas is traced by the Hβ line (*upper left-hand panel*) and is consistent with the predicted velocities of a massive rotating disk (lower left-hand panel; see § 4.2 for details), with 1 σ residual velocities of 8.5 km s^{-1} (*lower right-hand panel*). The high-excitation [O III]–emitting gas has a secondary velocity component consistent with the presence of large ($\sim$350 km s^{-1}) radial flows outside the plane of the rotating disk (*upper right-hand panel*).

axis oriented along P.A. 15° $\pm$ 10°. Both the amplitude and the P.A. of the kinematic axes indicate that the velocity field of this [O III] component is rather different from the low-ionization gas (Fig. 4, upper left-hand panel). In fact, the large velocities involved, as well as the different orientation of the kinematic major axis, strongly suggest that this high-ionization gas is flowing outside the low-ionization rotating gas disk (§ 4.3).

4. DISCUSSION

4.1. *Origin of the Activity in NGC 4303: The Starburst-AGN Connection*

The presence of nuclear star-forming regions in Seyfert galaxies is a well-established observational result (Pogge 1989; Gonzalez-Delgado & Pérez 1997). In some of these galaxies, the star-forming regions are located at distances of about a few to several hundred parsecs from the core, and they dominate the observed UV emission (Colina et al. 1997b; Gonzalez-Delgado et al. 1998). However, NGC 4303 represents the first active galaxy where nuclear star-forming regions are arranged in a spiral-like structure that can be traced all the way down into the unresolved UV-bright core (Colina et al. 1997a). The presence of this structure in the nuclear regions of NGC 4303 and its proximity (at a distance of 16.1 Mpc) make this galaxy a unique target for the study of the starburst-AGN connection in active galaxies.

The optical emission line diagnostic diagrams for the core of NGC 4303 and for the brightest nuclear star-forming regions are presented in Figure 5. The predicted emission line ratios for a solar metallicity instantaneous burst of stars as a function of age are also shown for the cases of a large diffuse ($N_e \sim 10^2$ cm^{-3}, with a radius of 70 pc) and a more dense and compact ($N_e \sim 10^3$ cm^{-3}, with a radius of 20 pc) star-forming region (M. García-Vargas 1997, private communication). In addition, the predicted emission line ratios for power-law models (Ho, Shields, & Filippenko 1993) covering a wide range of spectral indexes ($\alpha = -1$ to -2.5 for log $U = -2.5$) and ionization parameters (log $U = -2$ to -4 for $\alpha = -1.5$) are also indicated.

The optical emission line ratios measured in the nuclear star-forming regions (R1, R2, and R3 in Table 1) are consistent with those expected in an extremely young cluster of massive stars having ages between 2 and 3 Myr. Massive

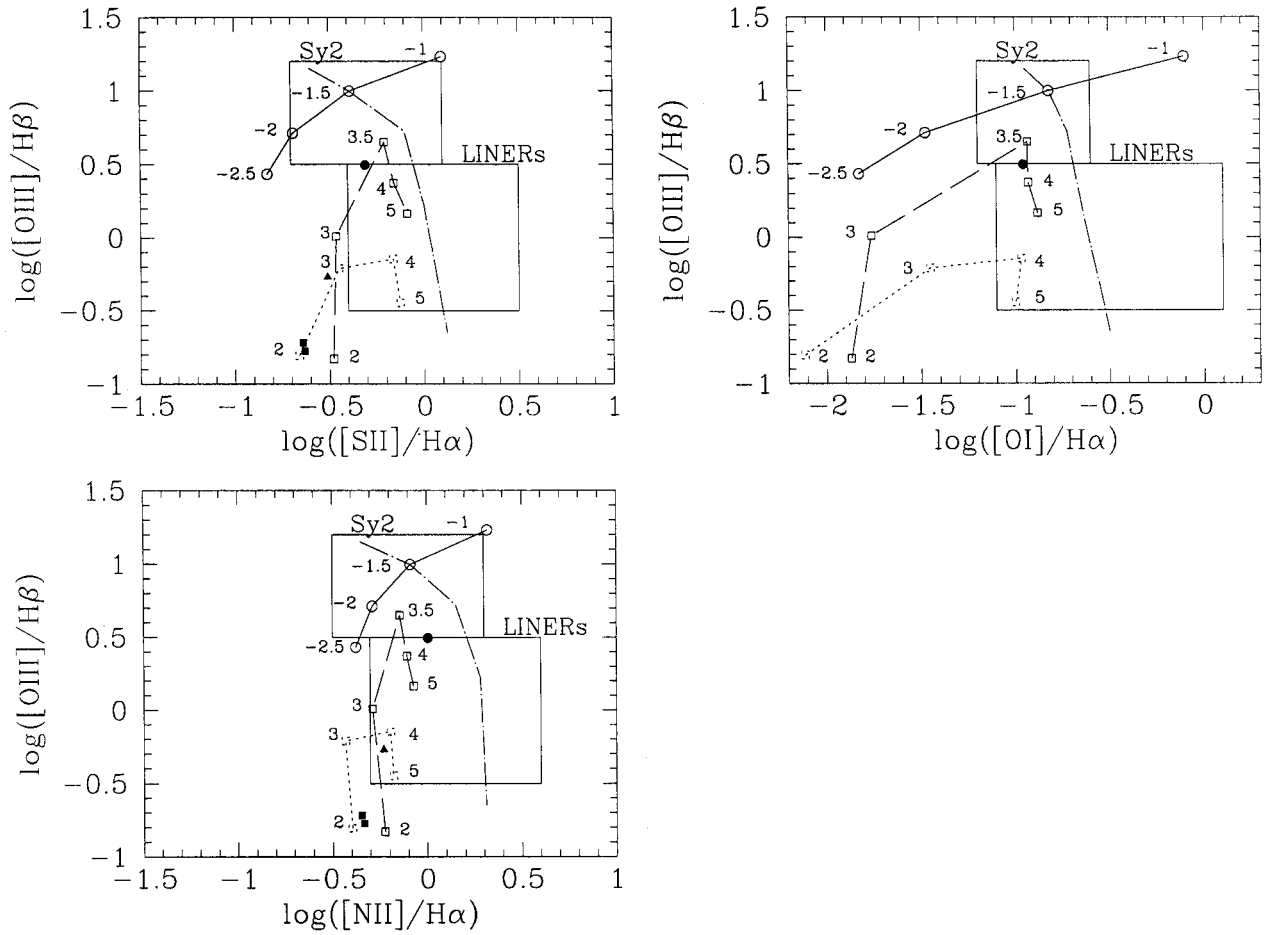

FIG. 5.—Emission-line excitation diagnostic diagrams showing the line ratios measured in the core of NGC 4303 (*filled circle*), the two brightest Hα-emitting regions surrounding it (*filled squares*), and the integrated core plus nuclear regions (*filled triangle*). The predicted emission line ratios for dense compact ($N_e = 10^3$ cm^{-3}, $r = 20$ pc) and large diffuse ($N_e = 10^2$ cm^{-3}, $r = 70$ pc) aging stellar clusters are plotted (dashed and dotted lines, respectively). The numbers indicate the age of the cluster in units of Myr. The predicted emission line ratios for a nonthermal ionization source covering a range of spectral indexes ($\alpha = -1$ to -2.5 for log $U = -2.5$) and ionization parameters (log $U = -2$ to -4 for $\alpha = -1.5$) are also presented (solid and dot-dashed lines, respectively). Boxes covering the observed range of emission-line ratios for Seyfert 2 galaxies and LINERs are indicated.

main-sequence stars of about 30 $M_\odot$ or more evolve toward the supergiant phase in about 5 Myr, and if red supergiants were present in the nuclear star-forming regions of NGC 4303, they would be dominating the red and near-infrared flux (Mas-Hesse & Kunth 1991). The nuclear star-forming regions in NGC 4303 are only detected in the UV continuum and in the ionized gas, but not in the optical and near-infrared continuum, which gives further support to the idea that these clusters are young and that the massive stars have not yet evolved into the red supergiant phase; i.e., no contribution to the optical and near-infrared continuum from stars older than 5 Myr is significant in these regions.

The optical emission line ratios associated with the core of NGC 4303 have values between those of low-excitation Seyfert 2 and LINERs. Traditionally, these ratios have been considered as direct tracers of a power-law nonthermal ionizing source associated with the emission of an accretion disk around a black hole (see Fig. 5 for optical emission line ratios predicted by a power-law ionization source). This scenario has recently been challenged by the detection of spectral feature characteristics of clusters of massive young stars in the UV spectra of several UV-bright LINERs (Maoz et al. 1998) and Seyfert 2 galaxies (Heckman et al. 1997; Gonzalez-Delgado et al. 1998). Moreover, these clusters of young massive stars are the dominating ionizing sources in the nuclear regions of several Seyfert 2 galaxies (Colina et al. 1997b; Heckman et al. 1997; Gonzalez-Delgado et al. 1998).

Without the benefit of a UV spectrum, the nature of the UV-bright ionizing source located at the core of NGC 4303 is still unclear. The core of NGC 4303 can be classified as a [O I]–weak LINER. The optical emission line ratios in this subclass of LINERs are consistent with gas being ionized by a young massive star cluster located at the core of these galaxies (Filippenko & Terlevich 1992; Shields 1992). The upper limit to the size of the UV-bright core in NGC 4303 (8 pc in diameter from *HST* observations; Colina et al. 1997a), its observed UV luminosity [log $L_{\rm UV}(2200) = 37.79$ ergs s^{-1} Å^{-1}; Colina et al. 1997a], its Hα luminosity [log $L(\mathrm{H}\alpha) = 39.2$ ergs s^{-1} obtained from Keel 1983, converting to a distance of 16.1 Mpc and assuming the core generates 10% of the total Hα luminosity], and the optical emission line ratios are consistent with the existence of a cluster of young stars characterized by a mass of ~ 5–8×10^4 $M_\odot$ and an age of about 3.5–4 Myr (see Fig. 5).

On the other hand, the ratio of the UV to Hα flux observed in the nuclear star-forming regions and in the core of the galaxy (see ratios in Table 1) could also indicate the

presence of an ionization mechanism other than stars operating at the core of the galaxy. As mentioned earlier (§ 3.2), while the core is a factor of 2 brighter than the brightest nuclear star-forming regions, the converse is true for the Hα emission. Models of power laws and aging starbursts (Colina et al. 1997b) predict that for a given Hα luminosity and in the absence of extinction, the UV (2200 Å) luminosity of a power-law ionizing source is about 1.5–2.5 times that of a young starburst. However, differential extinction could play a relevant role in diminishing the observed UV luminosity of the nuclear star-forming regions relative to the UV-bright core.

No matter what the nature of the ionizing central source is, the nuclear star-forming regions of NGC 4303 are the major contributors to the total ionizing luminosity emitted in the nuclear regions of this galaxy. NGC 4303 is therefore an example of an active galaxy classified as a [O I]–weak LINER or low-excitation Seyfert 2, where the ionizing flux is dominated not by the UV-bright unresolved source located at the core of the galaxy but by nuclear clusters of young stars.

4.2. *The Evidence for a Massive Nuclear Rotating Disk in NGC 4303*

In § 3.3 it was shown that the kinematic and photometric major axes of the ionized gas agree with the major axis of the UV light distribution (see Figs. 3 and 4). This result strongly suggests that gas and stars are located in a disk that rotates around the center of the galaxy. While the morphology of the UV-emitting regions is compatible with a ringlike structure, the [S II] λλ6717, 6731 line intensity map shows a low surface brightness diffuse ionized gas uniformly distributed within the inner 2.″5 in radius (Fig. 3), therefore reinforcing the existence of a disk.

To analyze how well the observed velocity field could be represented by a rotating disk, a simple kinematic model (Mihalas & Binney 1981) is fitted to the data: $v_r(R, \theta) = V_{sys} + Z(R) \times \cos i + \Omega(R) \times \cos [\theta - \delta(R)] \times \sin i$, where V_{sys} is the systemic velocity, $\Omega(R)$ is the amplitude of the velocity field projected on the galactic plane, $Z(R)$ is a hypothetical perpendicular component, and $\delta(R)$ is the P.A. of the kinematic major axis, which can change with the distance from the center. R and θ are the galactocentric polar coordinates in the plane of the galaxy. To perform the fit, we interpolate elliptical rings—defined from the inclination of the galaxy ($i = 45°$) and from a first estimation of the P.A. of the kinematic major axis (P.A. $\sim$ 135 °, photometric major axis)—on the projected velocity field.

It is interesting to note that the values of the quantity $V_{sys} + Z(R) \times \cos i$ obtained by the model are nearly constant over the measured distances and close to the systemic velocity determined from radio measurements. This indicates that the velocity component perpendicular to the plane of the disk should be very small. Assuming it is negligible, the model gives a mean value of 1552 km s^{-1} for V_{sys}, which is in somewhat better agreement with radio measurements (1569 $\pm$ 3 km s^{-1}) than the radial velocity of the core as defined by the peak of the Hβ emission. The P.A. of the kinematic major axis can also be considered constant, taking into account that for small radii, say $r < 2''$, the uncertainty in the determination of $\delta(R)$ is largely due to the limited sampling. On the other hand, the variation of Ω with radius indicates a nearly solid body rotation. $\Omega(R)$ was also obtained fixing $V_{sys} + Z(R) \cos i = 1552$ km s^{-1} and $\delta(R) = 315°$ (pure rotation in a plane disk) obtaining basically the same conclusions.

Using the output parameters of the model described above, the predicted Hβ velocity field (Fig. 5, lower left-hand panel) and residual velocities (i.e., observed-predicted; Fig. 5, lower right-hand panel) are computed. The velocity residuals with an rms of 8.5 km s^{-1} indicate that the model of a rotating disk well represents the observed velocity field of the low-ionization gas. The fact that the residual velocities do not correlate with the morphology of the line-emitting nuclear regions also suggests that no large ($\geq$10 km s^{-1}) measurable radial velocities exist in the Hβ-emitting gas.

The gravitational mass of the rotating disk can be computed by taking the results of the model fitted to the observed velocity field. For a deprojected rotation velocity of 85 km s^{-1} at a radius of 300 pc, the dynamical mass corresponds to 5.0×10^8 $M_\odot$, making the disk of NGC 4303 one of the most massive and compact nuclear disks detected to date in nearby active galaxies.

4.3. *The Massive Nuclear Disk in NGC 4303 and the Fueling of Active Galaxies*

According to theoretical scenarios (SFB89; SBF90), bars in spiral galaxies are an efficient mechanism for channeling gas from the outer to the nuclear regions. If ILRs exist, gas will pile up at the radii of the resonances, and star-forming rings will be formed. However, following the SFB89 and SBF90 scenarios, if no ILRs exist, the gas could settle into a nuclear disk of gas. If this disk were massive enough with a large fraction of the dynamical mass in the form of cold gas, further instabilities will take place and the gas will continue to flow inward with a configuration resembling a spiral. In this type of scenario, the degree to which the system forms stars before the gas reaches the center determines whether the principal form of activity is a starburst or an AGN.

The active galaxy NGC 4303 is a prime candidate for the type of scenario sketched above. NGC 4303 is a spiral galaxy classified as SAB(rs)bc (de Vaucouleurs et al. 1991), where the compact star-forming spiral-like structure is embedded in a massive nuclear disk of about 300 pc in radius and dynamical mass $\sim 5.0 \times 10^8$ $M_\odot$. NGC 4303 shows both starburst and AGN activity, while the former is the dominant source contributing to $\sim$90% of the Hα luminosity.

The star formation rate (SFR) and ionized gas mass involved in the nuclear disk can be estimated from the Hα luminosity by assuming a Salpeter IMF with masses in the 0.1–100 $M_\odot$ mass range and an average electron density of 10^3 cm^{-3}, and considering that only 50% of the available ionizing photons are used in the ionization of the gas while the rest are absorbed by the associated dust or escape. Under these assumptions, the SFR and ionized gas mass correspond to ~ 0.2 $M_\odot$ yr^{-1} and $\sim 5 \times 10^4$ $M_\odot$, respectively. The estimated SFR indicates that the system is transforming gas into stars rapidly before the gas reaches the core of the galaxy, and, therefore, under the SFB89 and SBF90 scenarios the principal form of activity is a starburst.

On the other hand, the estimated mass of ionized gas represents a small fraction ($\sim 10^{-4}$) of the dynamical mass of the nuclear disk, but most of this mass could still be in the form of cold gas as in many other nearby nuclear starburst galaxies where 20%–60% of the mass in the nuclear regions is in molecular gas (Kenney et al. 1992). Recent CO maps of

NGC 4303 indicate the presence of large amounts of molecular gas ($\sim 2 \times 10^9\ M_\odot$) within the inner 500 pc around the nucleus (Sofue et al. 1997).

Finally, it is relevant to mention here that the SFB89 and BSF90 scenarios do not take into account the effect that nuclear star-forming regions and a central AGN could have in the velocity field of the gas. Stellar wind– or AGN-related outflows could prevent the gas from flowing inward or could prevent the gas from collapsing and forming further stars. Evidence for large radial flows outside the plane of the disk already exists (see §§ 3.3 and 4.2), and velocity residuals obtained by applying a model of an inclined rotating disk place upper limits of ~ 10 km s^{-1} to the velocity of any radial flow (inward and/or outward) in the low-ionization gaseous rotating disk.

4.4. *Massive Nuclear Disks in NGC 4303 and Ultraluminous Infrared Galaxies*

The measured physical properties of the massive nuclear disk in NGC 4303 (with a radius of 300 pc and a dynamical mass of $5.0 \times 10^8\ M_\odot$) are in good agreement with the mass of $1.7 \times 10^9\ M_\odot$ of molecular gas measured inside a radius of 500 pc (Sofue et al. 1997). This result suggests that a large fraction of the mass in the nuclear disk of NGC 4303 can be in the form of molecular gas, and therefore self-gravity instabilities could play an important role in the formation of new stars and in the fueling of the central AGN (SFB89; Fukuda et al. 1999). Preliminary CO maps obtained with the Plateau de Bure millimeter interferometer indicate that the molecular gas is highly concentrated toward the center of the galaxy and shows the two-peak emission line profile characteristic of massive rotating disks. A full report of these results will be presented elsewhere.

The massive nuclear disk in NGC 4303 has physical properties similar to those inferred for the nuclear gas disks recently detected in ultraluminous infrared galaxies like Arp 220 (Scoville et al. 1997) and Mrk 231 (Bryant & Scoville 1996; Carilli, Wrobel, & Ulvestad 1998), which are characterized by a radius of about a few hundred parsecs and a mass of about $10^9\ M_\odot$ (Mrk 231) to $5.4 \times 10^9\ M_\odot$ (Arp 220). If the nuclear disks in these three galaxies share the same physical properties, their surface gas density and velocity dispersion would be similar, and therefore the disks would be subjected to the same kind of instabilities. If this were the case, since NGC 4303 is a factor of 5–10 closer than Arp 220 and Mrk 231, this galaxy would be an ideal laboratory to study in detail the structure and evolution of compact massive nuclear star-forming disks in active galaxies in general, and in ultraluminous infrared galaxies in particular.

However, there is a substantial difference between the star-forming disk in NGC 4303 and the nuclear star formation in the ultraluminous infrared galaxies mentioned above. While ultraluminous infrared galaxies like Arp 220 form stars at a rate of about 50–100 $M_\odot$ yr^{-1}, the corresponding star formation rate in the nuclear disk of NGC 4303 is almost 2 orders of magnitude smaller. It is not clear whether the large difference in the star formation rate is due to the nuclear disks being in a different evolutionary stage, or whether the presence of a nuclear bar like that in NGC 4303 (Colina & Wada 1999) is playing a major role in the formation of stars and in the ulterior evolution of the nuclear disk. These issues deserve further investigation with detailed models and high spatial resolution observations.

4.5. *Radial Flows and Ionization Cone in NGC 4303*

As already mentioned earlier (§ 3.3.2), the high-excitation [O III]–emitting gas has at least two major velocity components. The main component follows the rotational velocity pattern of the low-ionization gas. On the other hand, the secondary component is detected only in the inner $\sim 2''$ around the core of NGC 4303, has a velocity amplitude of ± 350 km s^{-1}, and has a kinematic major axis oriented along the minor axis of the massive rotating disk (see Fig. 4, upper panels).

Assuming that the spiral structure observed in the *HST* UV image is trailing, the nearest part of the massive rotating disk is oriented toward the northeast. Taking into account this geometry for the rotating disk, this [O III]–emitting gas traces ionized gas flowing radially outside the plane defined by the massive nuclear star-forming disk. The [O III]–emitting gas is most likely being directly ionized by the UV-bright source located at the core of the galaxy. Under this scenario, the redward radial component of the [O III]–emitting gas is obscured toward the northeast by the massive nuclear disk. This gives an explanation to the fact that this component is not clearly observed near the nucleus.

The geometry and the amplitude of these radial motions are reminiscent of the biconical, wind-related outflows observed in luminous infrared galaxies (Heckman, Armus, & Miley 1990; Colina, Lipari, & Macchetto 1991) or of the gas outflows observed along the ionization cone and radio jet axis in some Seyfert galaxies (Winge et al. 1997; Axon et al. 1998), but its precise nature is still unclear.

5. CONCLUSIONS

A detailed study of the nuclear region of the active galaxy NGC 4303 using two-dimensional spectroscopy with the 2D-FIS fiber system has been presented. The full potential of this powerful observing technique has been used to create continuum and emission-line maps of the nuclear region of NGC 4303, and to investigate in detail the excitation conditions and the velocity field of the ionized gas.

The main conclusions that can be drawn from this study are the following:

1. The observed velocity field of the ionized gas is consistent with the existence of a massive nuclear rotating disk. This disk is characterized by a dynamical mass of $5 \times 10^8\ M_\odot$, a radius of about 300 pc, an inclination of 45° with respect to the line-of-sight, and a spin axis along P.A. 40°.
2. The mass and size of the nuclear disk in NGC 4303 is within the range of the gas disks recently detected in the ultraluminous infrared galaxies Arp 220 and Mrk 231.
3. The UV-bright spiral structure detected with *HST* is embedded in the massive nuclear disk. Based on the optical emission line ratios, the nuclear UV-bright regions are consistent with being young (2–3 Myr) star-forming regions.
4. The nature of the UV-bright ionizing source located at the core of NGC 4303 is still unsolved. The observed properties of the core (size, optical emission line ratios, UV, and Hα luminosities) are consistent with the existence of a massive ($8 \times 10^4\ M_\odot$), young (3.5–4 Myr) stellar cluster, but the presence of a nonthermal power law AGN-like ionizing source cannot be ruled out.
5. NGC 4303 is another example of a low-luminosity active galaxy, where its ionization luminosity is dominated

by nuclear star-forming regions and not by the AGN-like unresolved source located at the core of the galaxy.

6. Large amplitude velocity (~ 350 km s^{-1}) outflows of gas outside the plane of the massive rotating disk are observed in the high-excitation [O III]–emitting gas. The velocity amplitude and geometry is reminiscent of the ionizing cones observed in many Seyfert galaxies.

The overall properties of the nuclear disk in NGC 4303 (with a radius of ~ 300 pc, mass of $5 \times 10^8\ M_\odot$, and a star formation rate of $\sim 0.2\ M_\odot\ \mathrm{yr}^{-1}$) and of its core (a LINER-type AGN contributing about 15% of the ionizing luminosity) makes this galaxy a candidate for the study of the AGN-starburst connection in active galaxies and for the investigation of AGN gas-fueling scenarios (SFB89; SBF90; Fukuda et al. 1999), where a massive nuclear disk with a large fraction of mass in the form of cold gas becomes gravitationally unstable, produces a gas inflow with a configuration resembling a spiral structure, and forms stars before the gas reaches the core of the galaxy. Detailed models involving the effects of stellar- or AGN-related winds are needed to compare in detail the evolution of massive nuclear gaseous disks with observational results like the ones presented in this paper.

We are grateful to M. García-Vargas for running the photoionization models for aging star clusters used in this paper and for helpful discussions. Thanks are due to A. García for his work on the development of the 2D-FIS system. We are also grateful to E. Mediavilla who participated in the design and commissioning phase of the 2D-FIS system.

REFERENCES

Arribas, S., Mediavilla, E., García-Lorenzo, B., & del Burgo, C. 1997, ApJ, 490, 227
Arribas, S., Mediavilla, E., & Rasilla, J. L. 1991, ApJ, 369, 260
Axon, D., Marconi, A., Capetti, A., Macchetto, F. D., Schreier, E., & Robinson, A. 1998, ApJ, 496, L75
Benedict, G. F., Smith, B. J., & Kenney, J. D. P. 1996, AJ, 112, 1318
Bryant, P. M., & Scoville, N. 1996, ApJ, 457, 678
Carilli, C. L., Wrobel, J. M., & Ulvestad, J. S. 1998, AJ, 115, 928
Carter, D., et al. 1993, User Manual XXIV (La Palma: ING)
Colina, L., & Wada, K. 1999, ApJ, submitted
Colina, L., García-Vargas, M. L., Mas-Hesse, J. M., Alberdi, A., & Krabbe, A. 1997a, ApJ, 484, L41
Colina, L., García-Vargas, M. L., González-Delgado, R. M., Mas-Hesse, J. M., Pérez, E., Alberdi, A., & Krabbe, A. 1997b, ApJ, 488, L71
Colina, L., Lípari, S., & Macchetto, F. D. 1991, ApJ, 379, 113
de Vaucouleurs, G., de Vaucouleurs, A., Corwin, H. G., Buta, R. J., Paturel, G., & Fouque, P. 1991, in Third Reference Catalogue of Bright Galaxies (Berlin: Springer)
Elmegreen, D. M., Chromey, F. R., Santos, M., & Marshall, D. 1997, AJ, 114, 1850
Ferrarese, L., et al. 1996, ApJ, 464, 568
Filippenko, A. V., & Sargent, W. L. W. 1986, in Structure and Evolution of Active Galactic Nuclei, ed. G. Giuricin, F. Mardirossian, M. Mezetti, & M. Ramella (Dordrecht: Reidel), 21
Filippenko, A. V., & Terlevich, R. 1992, ApJ, 397, L79
Fukuda, H., Wada, K., & Habe, A. 1999, MNRAS, submitted
García, A., Rasilla, J. L., Arribas, S., & Mediavilla, E. 1994, Proc. SPIE, 2198, 75
González-Delgado, R. M., Heckman, T., Leitherer, C., Meurer, G., Krolik, J., Wilson, A. S., Kinney, A., & Koratkar, A. 1998, ApJ, 505, 174
González-Delgado, R. M., & Pérez, E. 1997, ApJS, 108, 199
Heckman, T., Armus, L., & Miley, G. 1990, ApJS, 74, 833
Heckman, T., González-Delgado, R. M., Leitherer, C., Meurer, G. R., Krolik, J., Wilson, A. S., Koratkar, A., & Kinney, A. 1997, ApJ, 482, 114
Ho, L. C., Shields, J. C., & Filippenko, A. V. 1993, ApJ, 410, 567
Howarth, J. D., & Murray, J. 1988, Starlink User Note 50
Keel, W. C. 1983, ApJS, 52, 229
Kenney, J. D. P., Wilson, C. D., Scoville, N. Z., Devereux, N. A., & Young, J. S. 1992, ApJ, 395, L79
Kennicutt, R. C., Keel, W. C., & Blaha, C. A. 1989, AJ, 97, 1022
Knapen, J. H., Beckman, J. E., Heller, C. H., Shlosman, I., & de Jong, R. S. 1995, ApJ, 454, 623
Maoz, D., Koratkar, A., Shields, J. C., Ho, L. C., Filippenko, A., & Sternberg, A. 1998, AJ, 116, 55
Mas-Hesse, J. M., & Kunth, D. 1991, A&AS, 88, 399
Mihalas, D., & Binney, J. 1981, Galactic Astronomy, Structure, and Kinematics (2d ed.; NewYork: Freeman)
Norman, C., & Scoville, N. 1988, ApJ, 332, 124
Pogge, R. W. 1989, ApJS, 71, 433
Scoville, N. Z., Yun, M. S., & Bryant, P. M. 1997, ApJ, 484, 702
Shapiro, S., & Teukolsky, S. A. 1985, ApJ, 292, L41
Shields, J. C. 1992, ApJ, 399, L27
Shlosman, I., Begelman, M., & Frank, J. 1990, Nature, 345, 679 (SBF90)
Shlosman, I., Frank, J., & Begelman, M. C. 1989, Nature, 338, 45 (SFB89)
Sofue, Y., Tutui, Y., Honma, M., & Tomita, A. 1997, AJ, 114, 2428
Terlevich, R., Tenorio-Tagle, G., Franco, J., & Boyle, B. 1994, in Nature of Compact Objects in AGNs, ed. A. Robinson & R. Terlevich (Cambridge: Cambridge Univ. Press), 209
Weedman, D. 1983, ApJ, 266, 479
Winge, C., Axon, D. J., Macchetto, F. D., & Capetti, A. 1997, ApJ, 487, L121